Magnetic fields in normal galaxies

Rainer Beck

Phil. Trans. R. Soc. Lond. A 2000 **358**, 777-796
doi: 10.1098/rsta.2000.0558

THE ROYAL SOCIETY

PHILOSOPHICAL TRANSACTIONS OF THE ROYAL SOCIETY A MATHEMATICAL, PHYSICAL & ENGINEERING SCIENCES

Magnetic fields in normal galaxies

By Rainer Beck

Max-Planck-Institut für Radioastronomie,
Auf dem Hügel 69, D-53121 Bonn, Germany

Linearly polarized radio continuum emission is a powerful tool for studying the strength and structure of interstellar magnetic fields in galaxies. Interstellar magnetic fields with a well-ordered spiral structure exist in grand-design, flocculent and even irregular galaxies. In grand-design galaxies the fields are aligned parallel to the optical spiral arms, but the strongest regular fields are found in interarm regions, sometimes forming 'magnetic spiral arms' between the optical spiral arms. Processes related to star formation tangle the field in the spiral arms. Faraday rotation of the polarization vectors shows patterns which support the existence of coherent large-scale fields in galactic discs. In a few galaxies an axisymmetric spiral pattern dominates, while others host a bisymmetric spiral field or a superposition of dynamo modes. In the majority of axisymmetric cases the field is directed inwards. In barred galaxies the magnetic field seems to follow the gas flow within the bar. The location of the shock front in the magnetic field deviates from that expected from hydrodynamical models. Within (and interior to) the circumnuclear ring the field is again of spiral shape, which leads to magnetic stresses, possibly driving gas inflow towards the active nucleus. The next-generation radio telescopes should be able to reveal the wealth of magnetic structures in galaxies.

Keywords: magnetic fields; polarization; dynamos; galaxies; spiral arms; interstellar medium

PHILOSOPHICAL TRANSACTIONS OF THE ROYAL SOCIETY A MATHEMATICAL, PHYSICAL & ENGINEERING SCIENCES

1. Radio polarization observations

Interstellar magnetic fields are illuminated by cosmic-ray electrons spiralling around the field lines, emitting synchrotron radiation, the dominant contribution to radio continuum emission at centimetre and decimetre wavelengths. Synchrotron emission is highly linearly polarized, intrinsically 70–75% in a completely regular magnetic field. The observable degree of polarization in galaxies is reduced by Faraday (wavelength-dependent) depolarization in magnetized plasma clouds, by geometrical (wavelength-independent) depolarization due to variations of the magnetic-field orientation across the telescope beam and along the line of sight, and by a contribution of unpolarized thermal emission (on average 10–20% at centimetre wavelengths, up to 50% locally). Typical fractional polarizations in galaxies are less than a few per cent in central regions and spiral arms, but 20–40% in-between the spiral arms and in outer regions. Thus, polarized radio intensities are weak, and only the largest telescopes are sufficiently sensitive to detect them (figure 1). The Effelsberg 100 m single-dish telescope provides an angular resolution of $1'\!.2$ at $\lambda 2.8$ cm (figure 2). Interferometric (synthesis) telescopes (VLA, ATCA, WSRT) offer higher angular resolution but miss

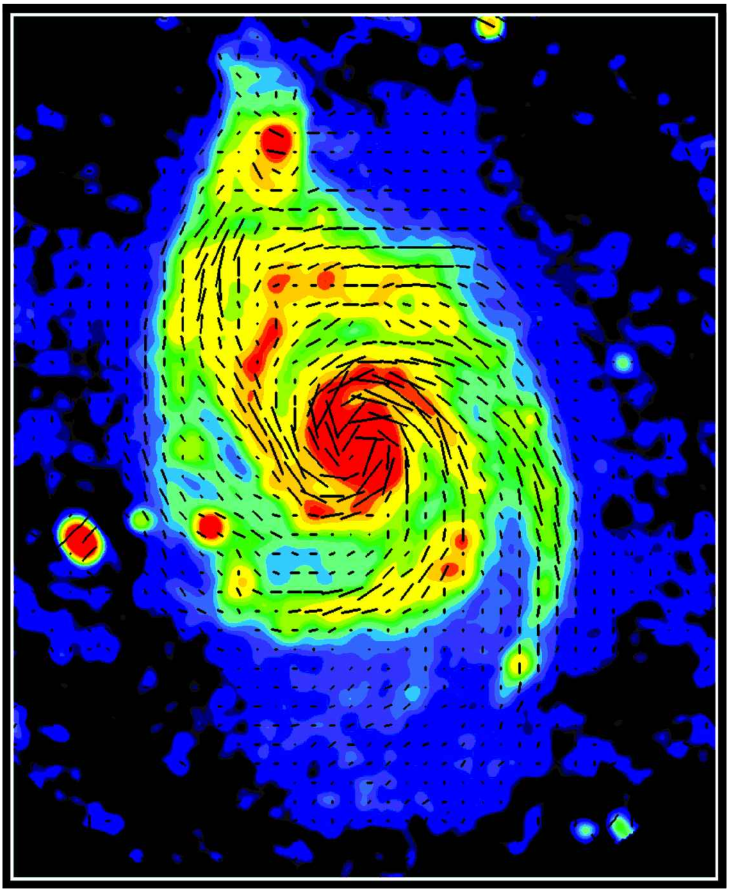

Figure 1. Total radio emission of M51 and B vectors of polarized emission at $\lambda 6.2$ cm (VLA ($15''$ synthesized beam), combined with the extended emission observed with the Effelsberg 100 m telescope ($2'.5$ resolution). The length of B vectors is proportional to polarized intensity. Faraday rotation has not been corrected as it is below 10° (Beck *et al.* 2000). (Copyright: MPIfR Bonn, R. Beck, C. Horellou and N. Neininger.)

large-scale structures in extended objects like nearby galaxies. Missing flux density in Stokes Q and U maps leads to wrong polarization angles. Combination of single-dish and synthesis data in all the Stokes parameters is required, at least for nearby galaxies (figures 1, 3 and 4).

At decimetre wavelengths Faraday depolarization significantly affects the transparency of the galactic discs to polarized radio waves (Sokoloff *et al.* 1998) so that only an upper part of the disc can be observed at these wavelengths (see, for example, Ehle & Beck 1993; Neininger *et al.* 1993). Large regions of a galaxy can be depolarized completely (Urbanik *et al.* 1997). At centimetre wavelengths the radio astronomer gets a clearer view of galactic magnetic fields. Faraday rotation of the polarization vectors becomes negligible below *ca.* $\lambda 3$ cm so that the B vectors (i.e. the observed E vectors rotated by 90°) directly trace the *orientation* of the regular field in the sky plane. The sign of Faraday rotation gives the *direction* of the field component along the line of sight. Typical interstellar rotation measures of *ca.* 50 rad m^{-2} lead to 10° rotation at λ6 cm and 3° at λ3 cm. To detect smaller rotation measures, observations at larger wavelengths, but still in the Faraday-thin regime, are required, e.g. $\lambda \approx 13$ cm. Such systems are available at the Effelsberg, ATCA and WSRT telescopes, but not yet at the VLA.

Tables 1 and 2 give a summary of the available radio polarization data.

2. Magnetic-field strengths

The average 'equipartition' strength of the total $\langle B_{\mathrm{tot},\perp}\rangle$ and the resolved regular field $\langle B_{\mathrm{reg},\perp}\rangle$ *in the plane of the sky* can be derived from the total and polarized radio synchrotron intensity, respectively, if energy-density equipartition between cosmic rays and magnetic fields or minimum total energy density is assumed. Furthermore, the ratio between cosmic-ray protons and electrons K (and its variation with particle energy), the synchrotron spectral index α, the extent of the radio-emitting region along the line of sight and the volume filling factor of the field have to be known. Fortunately, the derived equipartition field strength depends on the power $1/(\alpha+3)$ of each of these parameters so that even large uncertainties lead to only moderate errors in field strength.

The standard minimum-energy formulae generally use a fixed integration interval in radio *frequency* to determine the total energy density of cosmic-ray electrons. This procedure makes it difficult to compare minimum-energy field strengths between galaxies because a fixed frequency interval corresponds to different electron energy intervals, depending on the field strength itself. When instead a fixed integration interval in *energy* is used, the minimum energy and energy equipartition estimates give similar values for $\langle B_{\mathrm{tot},\perp}^{3+\alpha}\rangle$, where α is typically approximately equal to 0.9. The resulting estimate of $\langle B_{\mathrm{tot},\perp}^{3+\alpha}\rangle^{1/(3+\alpha)}$ is larger than the mean field $\langle B_{\mathrm{tot},\perp}\rangle$ if the field strength varies along the path length. If, on the other hand, the field is concentrated in filaments with a volume filling factor f, the equipartition estimate is smaller than the field strength in the filaments by a factor $f^{1/(3+\alpha)}$ (see Beck *et al*. 1996).

The mean magnetic-field strength for the sample of 74 spiral galaxies observed by Niklas (1995) is $\langle B_{\mathrm{tot},\perp}\rangle = 9\,\mu\mathrm{G}$ (0.9 nT) with a standard deviation of 3 μG, using $K = 100$. In nearby galaxies the average total field strengths in the galactic plane (corrected for inclination) range between $\langle B_{\mathrm{tot}}\rangle \simeq 4\,\mu\mathrm{G}$ in M33 (Buczilowski & Beck 1991) and $\simeq 15\,\mu\mathrm{G}$ in M51 (Neininger 1992). In spiral arms the total field strengths can reach *ca.* 20 μG locally, like in NGC 6946 (Beck 1991), M51 and M83. Interacting galaxies host even stronger magnetic fields, probably larger than the equipartition values (Hummel & Beck 1995). The strongest field within a normal galaxy found so far is that in the circumnuclear ring of NGC 1097 with $B_{\mathrm{tot}} \simeq 40\,\mu\mathrm{G}$ (Beck *et al*. 1999).

The strengths of the resolved regular fields B_{reg} are typically 1–5 μG locally, but *ca.* 13 μG in an interarm region of NGC 6946 (Sect. 5); these are always lower limits due to the limited angular resolution.

3. Magnetic fields and gas clouds

Comparison of the maps of the total radio emission of M51 (figure 1) with the total (cold plus warm) dust emission (Block *et al*. 1997) reveals a surprisingly close

Table 1. *Radio polarization observations and magnetic field structures of normal galaxies with low or moderate inclination*

(Instruments: E, Effelsberg 100 m; A, Australia Telescope Compact Array; V, Very Large Array; P, Parkes 64 m; W, Westerbork Synthesis Radio Telescope. Notation: ASS, axisymmetric spiral structure ($m = 0$ dynamo mode) dominates; BSS, bisymmetric spiral structure ($m = 1$ dynamo mode) dominates; MSS, mixed modes.)

galaxy	wavelength (cm)	field structure	reference
M33	E 21, 18, 11, 6, 2.8	spiral, BSS?	Buczilowski & Beck (1991)
M51	W 21, 6		Segalovitz *et al.* (1976)
	E 6, 2.8	MSS, magnetoionic halo,	Berkhuijsen *et al.* (1997),
	V 20, 18, 6	interarm fields	Horellou *et al.* (1992), Neininger & Horellou (1996)
M81	E 6, 2.8	BSS (+weaker ASS),	Krause *et al.* (1989*b*), Sokoloff *et al.* (1992),
	V 20, 6	interarm fields	Schoofs (1992)
M83	E 6, 2.8	MSS and ‖ bar,	Neininger *et al.* (1991, 1993),
	V 20, 6		Sukumar & Allen (1989),
	A 13	magnetic arms	Ehle (1995), M. Ehle *et al.* (unpublished data)
M101	E 11, 6	spiral	Gräve *et al.* (1990), E. M. Berkhuijsen *et al.* (unpublished data)
NGC 1097	V 22, 18, 6, 3.5	‖ gas flow, nuclear spiral	Beck *et al.* (1999)
NGC 1365	V 22, 18, 6, 3.5	‖ gas flow	V. Shoutenkov *et al.* (unpublished data)
NGC 1559	A 13, 6	⊥ bar	M. Ehle *et al.* (unpublished data)
NGC 1566	A 20, 13, 6	spiral, interarm fields	Ehle *et al.* (1996)
NGC 1672	A 20, 13, 6	spiral, interarm fields	M. Ehle (unpublished data)
NGC 2276	V 20, 6	spiral, BSS?	Hummel & Beck (1995)
NGC 2403	E 11, 6		T. Pannuti *et al.* (unpublished data)
NGC 2442	A 13, 6	spiral, ‖ bar	M. Ehle *et al.* (unpublished data)
NGC 2903	E 6, 2.8	spiral	R. Beck (unpublished data)
	V 18, 20		
NGC 2997	V 20, 6, 3.5	spiral, ASS in inner region	Han *et al.* (1999*b*)
	A 13		

Table 1. *Cont.*

galaxy	wavelength (cm)	field structure	reference
NGC 3521	E 2.8	spiral	Knapik *et al.* (2000)
NGC 3627	E 2.8	‖ dust lane,	Soida *et al.* (1999),
	V 6, 3.5	anomalous magnetic arm	M. Soida *et al.* (unpublished data)
NGC 4038/39	V 20, 6, 3.6	‖ tidal arm	K. T. Chyzy *et al.* (unpublished data)
NGC 4254	E 6, 2.8	spiral, ‖ compression region	Soida *et al.* (1996)
	V 20, 6, 3.5		K. T. Chyzy *et al.* (unpublished data)
NGC 4258	W+V 21		van Albada & van der Hulst (1982),
	E 6, 2.8	‖ anomalous arms,	Krause *et al.* (1984),
	V 20, 6	planar spiral jet?	Hummel *et al.* (1989)
NGC 4414	V 6, 3.5	spiral, MSS?	M. Soida *et al.* (unpublished data)
NGC 4449	E 2.8, 6	‖ optical filaments,	Klein *et al.* (1996),
	V 6, 3.5	spiral	Chyzy *et al.* (2000)
NGC 4535	V 22, 18, 6, 3.5	spiral	V. Shoutenkov *et al.* (unpublished data)
NGC 5055	E 2.8	spiral, ‖ dust filaments	Knapik *et al.* (2000)
NGC 6822	E 6	isolated patches	J. Knapik *et al.* (unpublished data)
NGC 6946	E 11, 6, 2.8	spiral,	Ehle & Beck (1993),
	V 22, 18, 6, 3.5	MSS, magnetic arms	Beck & Hoernes (1996), R. Beck (unpublished data)
NGC 7479	V 22, 18, 6, 3.5	extraplanar spiral 'jet'?	V. Shoutenkov *et al.* (unpublished data)
NGC 7552	A 6	spiral, ⊥ bar	M. Ehle *et al.* (unpublished data)
IC 10	E 6	‖ local compression region	J. Knapik *et al.* (unpublished data)
IC 342	E 11, 6	ASS, magnetic spiral arms	Krause *et al.* (1989*a*), Sokoloff *et al.* (1992)
	V 20, 6, 3.5		R. Beck (unpublished data)
SMC	P 21, 12	‖ main ridge	Haynes *et al.* (1986)
LMC	P 21, 12, 6	loop south of 30 Dor	Haynes *et al.* (1991), Klein *et al.* (1993)

Table 2. *Radio polarization observations and magnetic field structures of (almost) edge-on galaxies*

(E, P, V, ASS: see table 1.)

galaxy	wavelength (cm)	field structure	reference
M31	E 21, 11, 6	ASS (+weaker BSS),	Beck (1982), Beck *et al.* (1989),
	V 20, 6	spiral (inner region)	Ruzmaikin *et al.* (1990), Beck *et al.* (1998)
M82	V 6, 3.6	halo, radial field	Reuter *et al.* (1994)
M104	V 20, 6	‖ disc	M. Krause *et al.* (unpublished data)
NGC 55	V 20		M. Soida *et al.* (unpublished data)
NGC 253	P 6		Harnett *et al.* (1990)
	V 20, 6	‖ plane, ASS	Carilli *et al.* (1992)
	E 6, 2.8	& spurs inclined to plane	Beck *et al.* (1994)
NGC 891	V 20, 6	‖ & spurs inclined to plane	Sukumar & Allen (1991)
	E 6, 2.8		Dumke *et al.* (1995),
	W 49		C. Debreuck *et al.* (unpublished data)
NGC 1808	V 20, 6	spurs ⊥ plane	Dahlem *et al.* (1990)
NGC 3079	V 6	extraplanar jet?	Duric & Seaquist (1988)
NGC 3628	V 20, 6	‖ plane,	Reuter *et al.* (1991),
	E 6, 2.8	spurs inclined to plane	Dumke *et al.* (1995)
NGC 4565	V 20, 6	‖ plane	Sukumar & Allen (1991),
	E 6, 2.8		Dumke *et al.* (1995)
NGC 4631	E 6, 2.8	‖ plane (outer region)	Hummel *et al.* (1991),
	V 6, 3.5	⊥ plane (inner region)	Golla & Hummel (1994)
	V 22, 18	halo, dipolar field	M. Krause *et al.* (unpublished data)
NGC 4666	V 20, 6	halo, field inclined to plane	Dahlem *et al.* (1997)
	E 6, 2.8		M. Dumke *et al.* (unpublished data)
NGC 4945	P 6	extensions ⊥ plane	Harnett *et al.* (1989)
NGC 5775	V 6	‖ plane	Golla & Beck (1990)
NGC 5907	V 20		
	E 6	‖ plane	M. Dumke & M. Krause (unpublished data)
NGC 7331	V 20, 6		E. Hummel (unpublished data),
	E 6, 2.8	almost ‖ plane	Dumke *et al.* (1995)
Circinus	A 13, 6	⊥ northern plume	Elmouttie *et al.* (1995)

connection. To understand its origin it is crucial to consider the strong (probably dominant) influence of the field strength on radio intensity. Magnetic fields are obviously anchored in gas clouds which are traced by the dust. Remarkably, one dust lane crosses the eastern spiral arm of M51, and so does the total field. Furthermore,

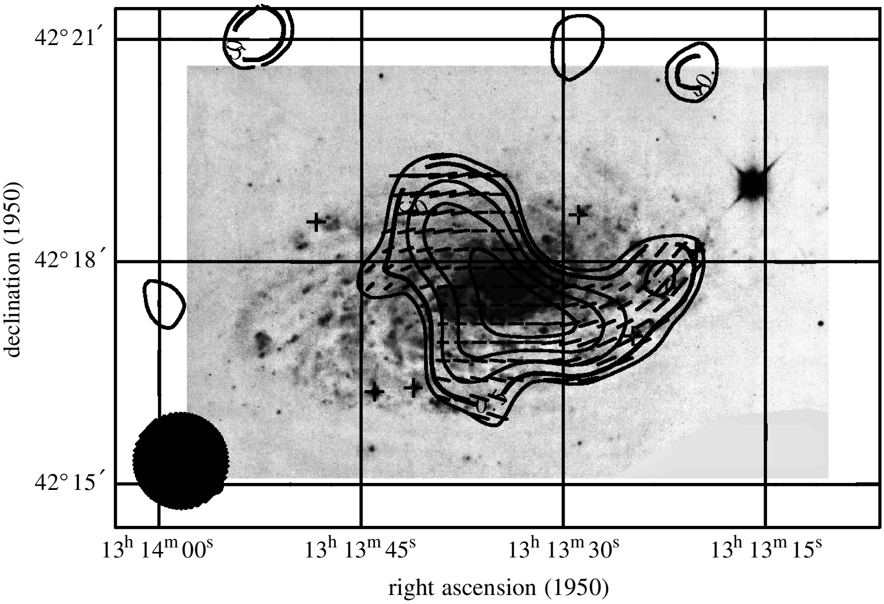

Figure 2. Polarized radio emission of the flocculent galaxy NGC 5055 at λ2.8 cm (Effelsberg 100 m telescope, 1′.2 resolution), superimposed onto an optical image from the *Carnegie atlas of galaxies*. The length of B vectors is proportional to polarized intensity (Knapik *et al.* 2000).

the total radio and far-infrared luminosities of galaxies are tightly correlated. Niklas & Beck (1997) explained the correlation, globally and locally and with the correct slope, by a close coupling of magnetic fields to gas clouds. The radio–far-infrared correlation within M31 indicates that the coupling is valid even for the more diffuse gas mixed with cool dust (Hoernes *et al.* 1998). The detailed comparison between the total synchrotron intensity and the cool gas ($HI + 2H_2$) in a spiral arm of M31 confirmed a coupling of the magnetic field to the gas (Berkhuijsen *et al.* 1993). The total field strength B_{tot} is high in spiral arms because the gas density is highest there.

The correlation between gas and *regular* fields is less obvious. Long prominent dust lanes are often connected to features of regular fields, e.g. in M83 (figure 3), in the anomalous arm of NGC 3627 (Soida *et al.* 1999) and in flocculent galaxies like NGC 5055 (figure 2). On the other hand, regular fields are sometimes observed in interarm regions with very little gas or dust (§ 5).

4. Magnetic-field structure

Grand-design spiral galaxies are shaped by density waves, but the role of magnetic fields is as yet unknown. Strong shocks should compress the magnetic field and increase the degree of radio polarization on the inner edges of the spiral arms. Radio observations, however, show a larger variety of phenomena.

The total radio intensity shows the total (i.e. regular plus random) field, while the polarized radio intensity shows the resolved regular field only. The strongest total and regular fields in M51 are found at the positions of the prominent dust lanes on the inner edges of the optical spiral arms (Neininger & Horellou 1996), as

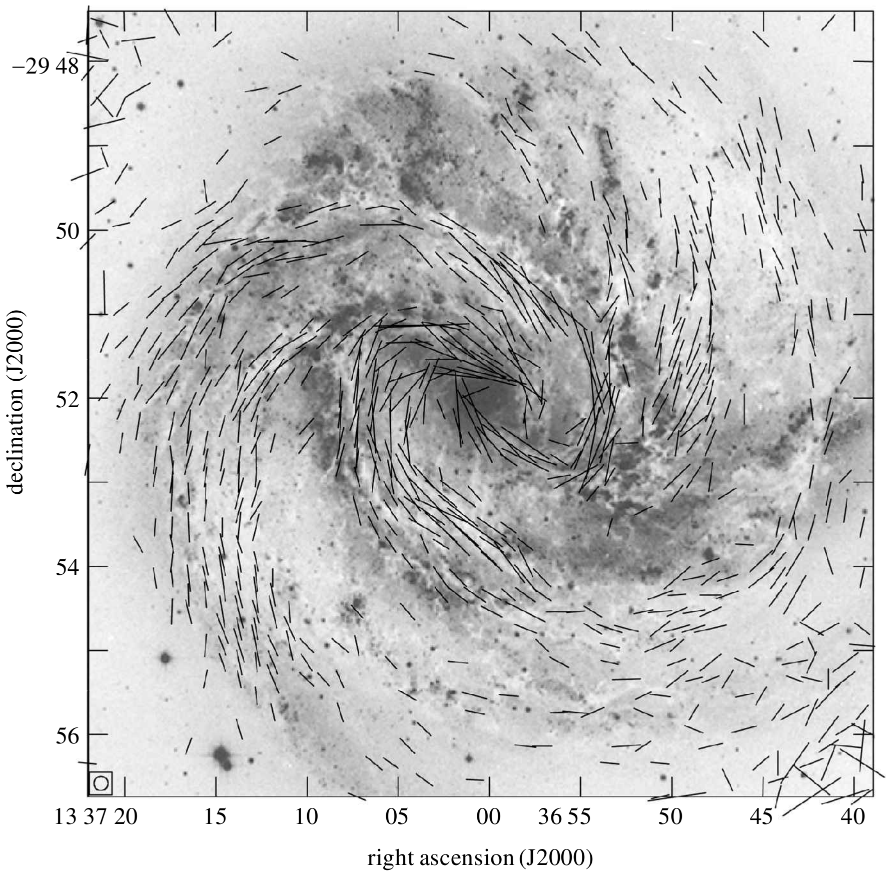

Figure 3. B vectors of polarized radio emission of M83 at λ6.2 cm (VLA, 10″ synthesized beam), combined with the extended emission observed with the Effelsberg 100 m telescope (2′.5 resolution), and superimposed onto an optical image of D. Malin (AAO). Faraday rotation has not been corrected as it is below 10°. The length of the B vectors is proportional to the polarized intensity (R. Beck, unpublished data).

expected from compression by density waves, but the regular fields extend far into the interarm regions. In NGC 2997 (Han *et al*. 1999*b*) and in M83 (figure 3) some of the polarized emission peaks at the inner edge of the optical arms, while the total emission shows no shift with respect to the optical arms. NGC 1566 (Ehle *et al*. 1996) and M81 (Krause *et al*. 1989*b*) show almost no signs of field compression; their strongest regular fields occur in *interarm regions*, while the total field is still highest in the optical spiral arms. Field tangling in the spiral arms, e.g. due to increased turbulent motions of gas clouds and supernova shock fronts, may explain this result (Sukumar & Allen 1989). In some cases, however, the interarm fields are concentrated in 'magnetic arms' which cannot be explained by the lack of field tangling (see § 5).

Radio polarization observations show that the B vectors of the regular fields largely follow the optical spiral structure in M51 (Neininger 1992; Neininger & Horellou 1996), M81 (Krause *et al*. 1989*b*; Schoofs 1992), M83 (Neininger *et al*. 1991, 1993;

Ehle 1995) and NGC 1566 (Ehle *et al*. 1996), though generally *offset* from the optical arms. In the density-wave picture the magnetic field is frozen into the gas clouds and is transported by the gas flow. Thus the field orientation should reflect the streaming lines of the gas, not the structure of the spiral wave itself. The pitch angles of the streaming lines are small in interarm regions and larger in spiral arms (though still smaller than those of the spiral wave). However, the observed pitch angles of the regular field are larger than those of the streaming lines almost everywhere. In the interarm regions of NGC 6946 the field pitch angle is *ca.* 20° (Rohde *et al*. 1999), while the gas flow is almost azimuthal. Hence, the regular magnetic field is not frozen into the gas flow, but probably modified by turbulent diffusion (von Linden *et al*. 1998) and/or shaped by dynamo action (§ 6).

Regular spiral magnetic fields with strengths similar to those in grand-design galaxies have been detected in flocculent galaxies (figure 2) and even in irregular galaxies (figure 4). The mean degree of polarization (corrected for different spatial resolutions) is similar between grand-design and flocculent galaxies (Knapik *et al*. 2000). Apparently, density waves have a relatively small effect on the field structure.

In our galaxy several field reversals between the spiral arms, on kpc scales, have been detected from pulsar rotation measures (Lyne & Smith 1989; Han *et al*. 1999*a*). Polarization observations of some external galaxies have sufficiently high spatial resolution, but similar reversals have not yet been detected in the maps of rotation measures, e.g. within the main emission 'ring' of M31 (figure 5). For other galaxies like M51, M83 and NGC 6946, the evidence against reversals is weaker but still significant. Field reversals may occur preferably in galaxies with less-organized spiral structure. Another explanation is that pulsar RMs in the galaxy trace the field near the galactic plane while RMs in external galaxies show the average regular field along the path length through the 'thick disc' (see § 7).

There is increasing observational evidence that magnetic fields are important for the formation of spiral arms. The streaming velocity and direction of gas clouds and their collision rates can be modified. Furthermore, magnetic fields will also influence the star-formation rates in spiral arms. Magnetic fields are essential for the onset of star formation as they allow the removal of angular momentum from the protostellar cloud during its collapse. Strong fields may also shift the stellar mass spectrum towards the more massive stars (Mestel 1994).

5. Magnetic spiral arms

Long arms of polarized emission were discovered in IC 342 (Krause *et al*. 1989*a*; Krause 1993). Observations of another gas-rich galaxy, NGC 6946 (Beck & Hoernes 1996), revealed a surprisingly regular distribution of polarized intensity with two 'magnetic arms' located in *interarm* regions, without any association with cool gas or stars, running parallel to the adjacent optical spiral arms. These magnetic arms do not fill the entire interarm spaces like the polarized emission in M81, but are only *ca.* 500–1000 pc wide. The fields in the magnetic arms must be *almost totally aligned*, and the peak strength of the regular field is *ca.* 13 μG. Recently, magnetic arms have also been found in M83 (figure 3, south of the bar) and in NGC 2997 (Han *et al*. 1999*b*).

The magnetic arms cannot be artefacts of depolarization. Firstly, their degree of polarization is exceptionally high (up to 50%). Secondly, they look quite similar at

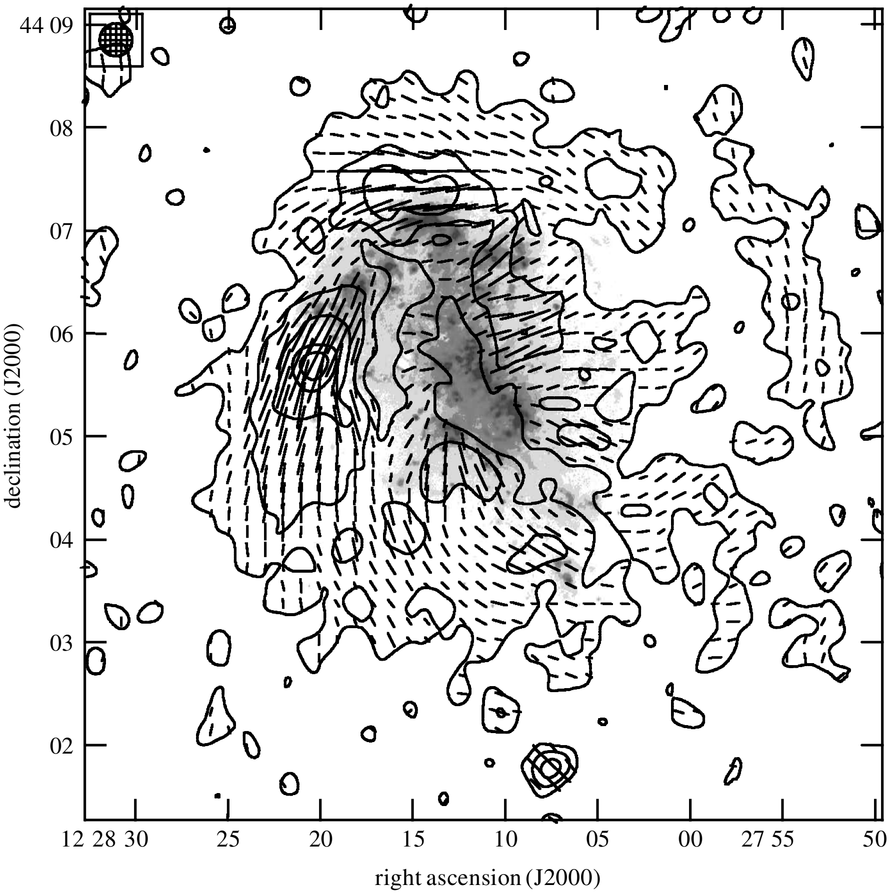

Figure 4. Polarized radio emission of the irregular galaxy NGC 4449 at λ6.2 cm (VLA, 19″ synthesized beam), combined with the extended emission observed with the Effelsberg 100 m telescope (2′.5 resolution), and superimposed onto an optical Hα image obtained by D. Bomans. The length of the B vectors is proportional to the polarized intensity (Chyzy *et al.* 2000).

λ6 cm and λ3 cm. Thirdly, they are also visible as peaks in total emission, which excludes their existence solely due to a window in geometrical depolarization (small field tangling).

We still do not understand how magnetic arms are generated. Fan & Lou (1997) suggested that they could be manifestations of slow MHD waves which may propagate in a rigidly rotating disc, with the maxima in field strength phase-shifted against those in gas density. However, all galaxies with magnetic arms rotate differentially beyond 1–2 kpc from the centre. Han *et al.* (1999*b*) found some correlation between the magnetic arms and interarm gas features generated in numerical models of perturbed galactic discs (Patsis *et al.* 1997). However, such models neglect the effect of magnetic fields. In dynamo models, using the reasonable assumption that the dynamo number is larger between the optical arms than in the arms (Shukurov 1998), magnetic arms evolve between the optical arms in a differentially rotating disc (Moss 1998; Rohde & Elstner 1998; Rohde *et al.* 1999). However, the back-reaction of

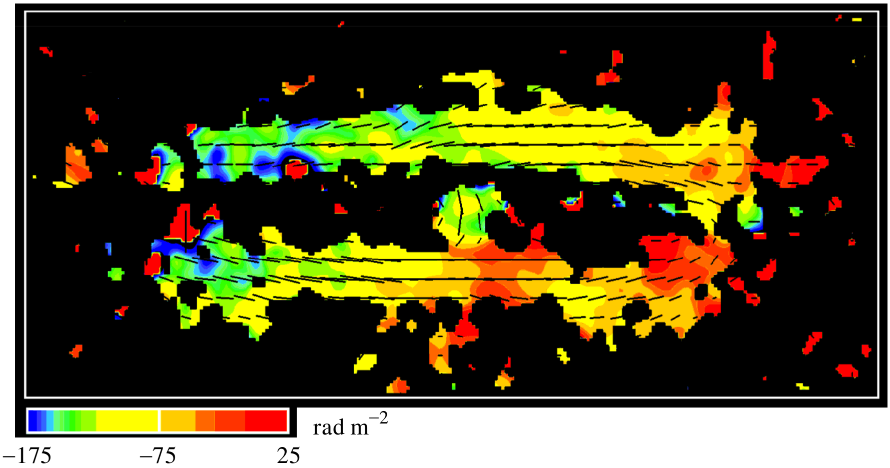

Figure 5. B vectors of the polarized radio emission of M31 at λ6.3 cm (Effelsberg 100 m telescope, smoothed to 5′ resolution), and rotation measures between λ6.3 cm and λ11.1 cm, obtained from Effelsberg data at 5′ resolution. The length of the B vectors is proportional to the polarized intensity (E. M. Berkhuijsen *et al.* (unpublished data)). (Copyright: MPIfR Bonn, R. Beck, E. M. Berkhuijsen and P. Hoernes.)

the field onto the gas has not been considered yet in present-day dynamo models. In the magnetic arms the energy density of the field may exceed that of the large-scale gas motion and thus distort the gas flow.

6. Faraday rotation and dynamos

Regular magnetic fields could in principle be shaped by gas flows and density waves. The B vectors of linearly polarized emission just indicate *anisotropy* of the magnetic-field distribution in the emission region. Imagine that a magnetic field without any regular structure (an isotropic random field) is compressed in one dimension by a shock. Emission from the resulting anisotropic field is linearly polarized with ordered B vectors, but the field is *incoherent*, i.e. it reverses its direction frequently within the telescope beam. Faraday *rotation measures* (RMs) are essential for distinguishing between coherent and incoherent fields. In an incoherent field the RMs are random and show no large-scale structure. Observation of RM *coherency* on a large scale, like in M31 (figure 5), NGC 6946 and NGC 2997 (Han *et al.* 1999*b*), means that the field was already coherent before compression, and hence there must be another physical mechanism (dynamo or primordial origin) to generate such an ordered field. The role of density waves would then be restricted to the alignment of the large-scale coherent field with the spiral arms.

The strongest evidence for dynamo action comes from M31 (figure 5). Radio observations of M31 revealed a 20 kpc-sized torus of magnetic fields aligned in *a single direction* (Beck 1982). Only a dynamo is able to generate a unidirectional field of such dimensions. RMs from polarized background sources confirmed this picture (Han *et al.* 1998). The regular field exists also interior to the prominent 'ring' and extends out to at least 25 kpc radius.

Dynamos are promising candidates for generating coherent fields, even in galaxies without density waves. The linear mean-field dynamo (e.g. Wielebinski & Krause 1993; Beck *et al*. 1996) generates magnetic-field modes which have spiral structure due to their azimuthal and radial field components. The pitch angle of the field spiral depends on the dynamo number, *not* on the pitch angle of the gas spiral. The field structure is described by modes of different azimuthal and vertical symmetry; in general a superposition of modes is generated. A large-scale pattern in maps of Faraday RMs reveals the dominance of a single dynamo mode (Krause 1990). A single-periodic azimuthal RM variation (with a phase equal to the pitch angle of the spiral structure) indicates a dominating axisymmetric dynamo mode (ASS, $m = 0$), as in M31 (figure 5; Beck 1982) and IC 342 (Krause *et al*. 1989*a*). Double-periodic azimuthal RM variations indicate a dominating bisymmetric dynamo mode (BSS, $m = 1$) if their phases vary with radial distance as expected (Krause 1990), as is the case for M81 (Krause *et al*. 1989*b*) and possibly M33 (Buczilowski & Beck 1991). The interacting galaxy M51 is a special case. Analysing all available polarization angle data, the field in M51 can be described as mixed modes (MSS), with axisymmetric and bisymmetric components having about equal weights in the disc, together with a horizontal axisymmetric halo field with opposite direction (Berkhuijsen *et al*. 1997). The magnetic arms of NGC 6946 may be the result of a superposition of the ASS and the quadrisymmetric ($m = 2$) modes, while the BSS mode is suppressed by the two-armed spiral structure of the gas (Rohde *et al*. 1999). In many other galaxies the data are still insufficient to allow a firm conclusion of whether the large-scale pattern of the regular field is even more complicated or the distribution of thermal gas is non-axisymmetric so that the RMs are distorted.

By comparing the signs of the RM distribution with the velocity field, inward and outward directions of the radial component of the spiral magnetic field can be distinguished. Surprisingly, all known ASS fields (M31, IC 342, NGC 253) and the MSS field in NGC 6946 point *inwards*. Dynamo action does not prefer one direction. This indicates some asymmetry in the initial seed field and excludes small-scale seed fields (Krause & Beck 1998), possibly a cosmologically relevant result.

The similarity of pitch angles between the dynamo-wave and the density-wave spiral is not self-evident and indicates the existence of some interaction between them. Future dynamo models have to include density waves and the back-reaction of the field.

7. Edge-on galaxies and radio halos

NGC 891, NGC 5907, NGC 7331 and other edge-on galaxies possess *thick radio discs* with *ca.* 1 kpc scale heights. In these galaxies the observed field orientations are mainly parallel to the disc (table 2). NGC 4565 has the most regular plane-parallel field (Sukumar & Allen 1991). The other extremes with *radio halos* with scale heights of several kpc are NGC 4631 (Hummel *et al*. 1991, figure 6) and NGC 253, the edge-on galaxy with the brightest and largest halo observed so far (Carilli *et al*. 1992). The irregular appearance of the NGC 253 halo is mainly due to the lower sensitivity compared with the map of NGC 4631. NGC 253 also has a bright X-ray halo so that a strong outflow from the disc or the nucleus driven by the high star-formation rate is probable. The regular magnetic field in the disc of NGC 253 is also predominantly parallel to the plane (Beck *et al*. 1994), which may be due to strong dynamo action even close to the centre. Some radio spurs with vertical field lines emerge from the outer disc. In contrast to the other radio-halo galaxies, the regular field of NGC 253 is also parallel to the plane in the lower halo, although the radio spectrum and the huge X-ray halo are clear indicators of a strong outflow.

Bright extended radio halos are rare. NGC 4631, NGC 4666 and M82 (Hummel *et al*. 1991; Dahlem *et al*. 1997; Reuter *et al*. 1994) are halo galaxies with dominating vertical field components. Magnetic spurs in these halos are connected to star-forming regions in the disc. The field is probably dragged out by the strong, inhomogeneous galactic wind. Dahlem *et al*. (1995) found evidence for a direct dependence of the halo extent on the level of energy input from the underlying disc. The magnetic-field lines in the NGC 4631 halo have a dipolar structure (figure 6) in the inner disc where differential rotation is weak, so the dipolar (antisymmetric) dynamo mode can evolve. A few regions with field orientations parallel to the disc are visible in the (differentially rotating) outer disc. Maps of rotation measures are required to test the dipolar model.

In the planes of edge-on spiral galaxies the observed polarized emission is weak due to depolarization effects. Faraday depolarization alone is insufficient to explain the low degrees of polarization near the plane of NGC 4631 (Golla & Hummel 1994). In their sample of edge-on galaxies, Dumke *et al*. (1995) found $p \simeq 5\%$ in the plane at $\lambda 2.8$ cm where Faraday effects are negligible. The field structure in the plane is mostly turbulent due to star-forming processes, causing depolarization along the line of sight as well as across the telescope beam. The degree of polarization at high frequencies increases with increasing distance from the plane because the star-forming activity and thus the field turbulence decrease.

8. Barred galaxies

Gas and stars in barred galaxies move in highly non-circular orbits. Gas streamlines are strongly deflected in the bar region along shock fronts, behind which the gas is compressed in a fast shearing flow (Athanassoula 1992). As the gas in the bar region rotates faster than the bar, compression regions traced by massive dust lanes develop along the edge of the bar that is leading with respect to the galaxy's rotation. Gas inflow along the compression region may fuel starburst activity in a dense ring near the galactic centre, although it is not clear how the gas can get rid of its angular momentum before falling into the active nucleus. The effects of magnetic fields on gas flows in barred galaxies have not yet been addressed in models.

From a sample of galaxies with strong optical bars observed with the Effelsberg, VLA and ATCA telescopes, the strongest regular magnetic fields were detected in NGC 1097, NGC 1365, NGC 4535 and NGC 7479. NGC 1097 and NGC 1365 are barred galaxies of morphological type SBbc with their bars lying almost in the plane of the sky so that spectroscopic observations of the shearing gas flow are very difficult.

The general similarity of the B vectors in NGC 1097 (figure 7) and gas streamlines around the bar as obtained in simulations (Athanassoula 1992) is striking. This suggests that the regular magnetic field is aligned with the shearing flow. We observe ridges of enhanced total magnetic fields which coincide with the optical dust lanes. The upstream and downstream regions of enhanced polarized emission are separated by a strip of zero polarized intensity, the location of the shock front, where the observed B vectors change their orientation abruptly (figure 7). This large deflection

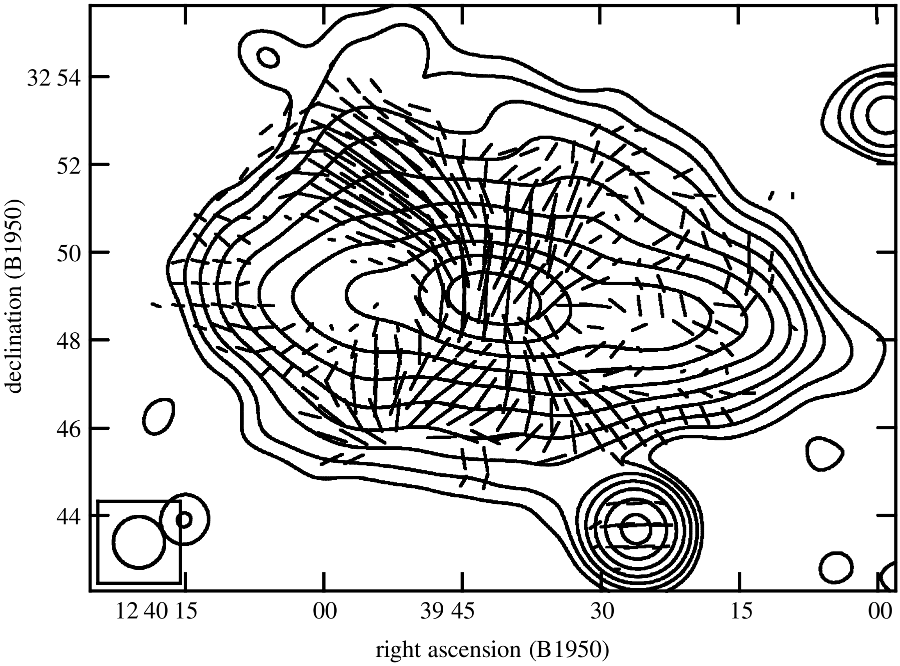

Figure 6. Total radio emission and B vectors of polarized emission of NGC 4631 at λ22 cm (VLA, 70″ synthesized beam). The B vectors have been corrected for Faraday rotation; their length is proportional to the polarized intensity (M. Krause *et al*. (unpublished data)).

angle leads to geometrical depolarization within the telescope beam because the strip where the field changes its direction is narrower than the spatial resolution of our observations. Our polarization observations imply that the shock front in the magnetic field is located 700–900 pc in front of the dust lanes, in contrast to conditions in classical shocks. Furthermore, the degree of field alignment is largest upstream (with a degree of polarization of up to 50%, right half of the bar in figure 7), not downstream. This indicates that the shock generates field turbulence. Numerical models including magnetic fields are required.

The circumnuclear ring of NGC 1097 is a site of ongoing intense star formation, with an active nucleus in its centre. The local equipartition strengths of the total and regular magnetic fields are $B_{tot} \simeq 40\,\mu G$ and $B_{reg} \simeq 7\,\mu G$ in the ring. The field strength reaches its absolute maximum where the compression region intersects with the ring. The regular field swings from alignment along the bar to a spiral pattern near the ring (Beck *et al*. 1999). In contrast to the bar, conditions for dynamo action are ideal in the ring. The orientation of the innermost field agrees with that of the spiral dust filaments visible in the optical HST image. Magnetic stress in the circumnuclear ring can drive mass inflow to feed the active nucleus in NGC 1097.

NGC 1365 is similar to NGC 1097 in its overall properties, but our polarization data indicate that the shearing flow in NGC 1365 is weaker. The compression of the magnetic field is only moderate, and we did not detect a region of strong field deflection. Instead, the field swings smoothly from outside into the bar, along with optical dust filaments.

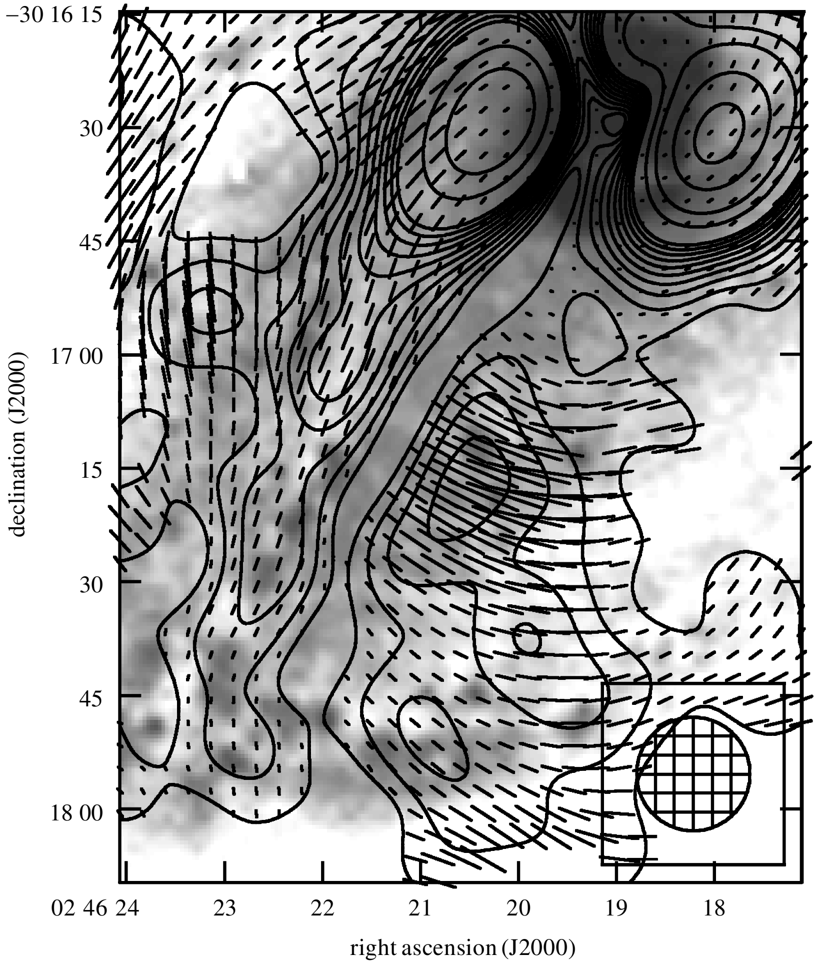

Figure 7. Total emission and B vectors of polarized radio emission of the southern half of the barred galaxy NGC 1097 at λ3.5 cm (VLA, 15″ synthesized beam), superimposed onto an optical image of H. Arp (MPE/Cerro Tololo). The length of B vectors is proportional to *the degree of polarization* (Beck *et al*. 1999).

Our results have revealed a principal difference between the behaviours of magnetic fields in barred and non-barred galaxies. In barred galaxies the magnetic field appears to interact strongly with the gas flow. In non-barred galaxies the field lines are of overall spiral shape so that the regular fields do *not* follow the gas flow, which is typical for dynamo-generated fields.

9. Nuclear outflows

NGC 7479 is another strongly barred apparently isolated spiral galaxy. A peculiar S-shaped region around the centre with 70″ (11 kpc) total projected extent was discovered in radio continuum at λ21 cm by Laine & Gottesman (1998). This feature has no counterpart in any other observed spectral range and it bends *opposite* to the optical spiral arms. The λ3.5 cm polarization data also revealed the 'jet', with the magnetic field oriented precisely parallel to this feature along its whole length. The strong and regular magnetic field suggests that nuclear activity may be driving it, as has been proposed for the jet in NGC 4258 (Hummel *et al*. 1989). A low-resolution λ22 cm polarization map indicates much stronger polarized intensity and significant Faraday rotation in the southern 'jet', giving evidence that the 'jet' was ejected out of the plane, similar to that in NGC 3079 (Duric & Seaquist 1988), while the jet of NGC 4258 is probably in the plane.

10. Open questions

The study of magnetic fields in galaxies is still in its infancy, in spite of the considerable progress achieved in recent years. Increasing resolution of the radio telescopes and higher sensitivity of the receiver systems revealed a spectrum of features: on the largest scales, extended spiral fields of different symmetry modes were found, typical signatures of dynamo action. How the field can adopt a similar pitch angle as that of the optical spiral remains a mystery. The preferred *inward* direction of axisymmetric fields, if confirmed by future observations, also awaits explanation. On intermediate scales, 'magnetic arms' between the optical spiral arms are still puzzling as they seem to be disconnected from the gas. On the other hand, fields can also be aligned by gas flows in density-wave and bar potentials. The unexpected location of the shock front in barred galaxies tells us that strong magnetic fields may interact with the gas flow, but details are still unobservable. Radio halos are the result of magnetic fields pulled outwards by galactic winds. (Or do dynamo-generated dipolar fields enhance the wind?) Some structures in radio halos show striking similarities to those in the solar corona: loops, spurs and possibly coronal holes.

All gas-rich galaxies, even irregular ones, host fields of *ca.* 1 nT strength. If the fields do not fill the whole interstellar space, they are even stronger. The dynamical importance of magnetic fields in galaxies can no longer be neglected. We are looking forward to the next generation of radio telescopes, with 100 times the sensitivity, which will present to us the full wealth of magnetic structures in galaxies.

References

Athanassoula, E. 1992 *Mon. Not. R. Astron. Soc.* **259**, 345.

Beck, R. 1982 *Astron. Astrophys.* **106**, 121.

Beck, R. 1991 *Astron. Astrophys.* **251**, 15.

Beck, R. & Hoernes, P. 1996 *Nature* **379**, 47.

Beck, R., Loiseau, N., Hummel, E., Berkhuijsen, E. M., Gräve, R. & Wielebinski, R. 1989 *Astron. Astrophys.* **222**, 58.

Beck, R., Carilli, C. L., Holdaway, M. A. & Klein, U. 1994 *Astron. Astrophys.* **292**, 409.

Beck, R., Brandenburg, A., Moss, D., Shukurov, A. & Sokoloff, D. 1996 *A. Rev. Astron. Astrophys.* **34**, 155.

Beck, R., Berkhuijsen, E. M. & Hoernes, P. 1998 *Astron. Astrophys. II* **129**, 329.

Beck, R., Ehle, M., Shoutenkov, V., Shukurov, A. & Sokoloff D. 1999 *Nature* **397**, 324.

Berkhuijsen, E. M., Bajaja, E. & Beck, R. 1993 *Astron. Astrophys.* **279**, 359.

Berkhuijsen, E. M., Horellou, C., Krause, M., Neininger, N., Poezd, A., Shukurov, A. & Sokoloff, D. 1997 *Astron. Astrophys.* **318**, 700.

Block, D. L., Elmegreen, B. G., Stockton, A. & Sauvage, M. 1997 *Astrophys. J.* **486**, L95.

Buczilowski, U. R. & Beck, R. 1991 *Astron. Astrophys.* **241**, 47.

Carilli, C. L., Holdaway, M. A., Ho, P. T. P. & de Pree, C. G. 1992 *Astrophys. J.* **399**, L59.

Chyzy, K. T., Beck, R., Kohle, S., Klein, U. & Urbanik, M. 2000 *Astron. Astrophys.* (In the press.)

Dahlem, M., Aalto, S., Klein, U., Booth, R., Mebold, U., Wielebinski, R. & Lesch, H. 1990 *Astron. Astrophys.* **240**, 237.

Dahlem, M., Lisenfeld, U. & Golla, G. 1995 *Astrophys. J.* **444**, 119.

Dahlem, M., Petr, M. G., Lehnert, M. D., Heckman, T. M. & Ehle, M. 1997 *Astron. Astrophys.* **320**, 731.

Dumke, M., Krause, M., Wielebinski, R. & Klein, U. 1995 *Astron. Astrophys.* **302**, 691.

Duric, N. & Seaquist, E. R. 1988 *Astrophys. J.* **326**, 574.

Ehle, M. 1995 PhD thesis, University of Bonn.

Ehle, M. & Beck, R. 1993 *Astron. Astrophys.* **273**, 45.

Ehle, M., Beck, R., Haynes, R. F., Vogler, A., Pietsch, W., Elmouttie, M. & Ryder, S. 1996 *Astron. Astrophys.* **306**, 73.

Elmouttie, M., Haynes, R. F., Jones, K. L., Ehle, M., Beck, R. & Wielebinski, R. 1995 *Mon. Not. R. Astron. Soc.* **275**, L53.

Fan, Z. & Lou, Y.-Q. 1997 *Mon. Not. R. Astron. Soc.* **291**, 91.

Golla, G. & Beck, R. 1990 In *The interstellar disk–halo connection* (ed. H. Bloemen), p. 47. Dordrecht: Kluwer.

Golla, G. & Hummel, E. 1994 *Astron. Astrophys.* **284**, 777.

Gräve, R., Klein, U. & Wielebinski, R. 1990 *Astron. Astrophys.* **238**, 39.

Han, J. L., Beck, R. & Berkhuijsen, E. M. 1998 *Astron. Astrophys.* **335**, 1117.

Han, J. L., Manchester, R. N. & Qiao, G. J. 1999*a* *Mon. Not. R. Astron. Soc.* **306**, 371.

Han J. L., Beck, R., Ehle, M., Haynes, R. F. & Wielebinski, R. 1999*b* *Astron. Astrophys.* **348**, 405.

Harnett, J. I., Haynes, R. F., Klein, U. & Wielebinski, R. 1989 *Astron. Astrophys.* **216**, 39.

Harnett, J. I., Haynes, R. F., Wielebinski, R. & Klein, U. 1990, *Proc. Astr. Soc. Australia* **8**, 257.

Haynes, R. F., Klein, U., Wielebinski, R. & Murray, J. D. 1986 *Astron. Astrophys.* **159**, 22.

Haynes, R. F. (and 11 others) 1991 *Astron. Astrophys.* **252**, 475.

Hoernes, P., Berkhuijsen, E. M. & Xu, C. 1998 *Astron. Astrophys.* **334**, 57.

Horellou, C., Beck, R., Berkhuijsen, E. M., Krause, M. & Klein, U. 1992 *Astron. Astrophys.* **265**, 417.

Hummel, E. & Beck, R. 1995 *Astron. Astrophys.* **303**, 691.

Hummel, E., Krause, M. & Lesch, H. 1989 *Astron. Astrophys.* **211**, 266.

Hummel, E., Beck, R. & Dahlem, M. 1991 *Astron. Astrophys.* **248**, 23.

Klein, U., Haynes, R. F., Wielebinski, R. & Meinert, D. 1993 *Astron. Astrophys.* **271**, 402.

Klein, U., Hummel, E., Bomans, D. J. & Hopp, U. 1996 *Astron. Astrophys.* **313**, 396.

Knapik, J., Soida, M., Dettmar, R.-J., Beck, R. & Urbanik, M. 2000 *Astron. Astrophys.* (In the press.)

Krause, F. & Beck, R. 1998 *Astron. Astrophys.* **335**, 789.

Krause, M. 1990 In *Galactic and intergalactic magnetic fields* (ed. R. Beck, P. P. Kronberg & R. Wielebinski), p. 187. Dordrecht: Kluwer.

Krause, M. 1993 In *The cosmic dynamo* (ed. F. Krause, K. H. Rädler & G. Rüdiger), p. 305. Dordrecht: Kluwer.

Krause, M., Beck, R. & Klein, U. 1984 *Astron. Astrophys.* **138**, 385.

Krause, M., Hummel, E. & Beck, R. 1989*a* *Astron. Astrophys.* **217**, 4.

Krause, M., Beck, R. & Hummel, E. 1989*b* *Astron. Astrophys.* **217**, 17.

Laine, S. & Gottesman, S. T. 1998 *Mon. Not. R. Astron. Soc.* **297**, 1041.

Lyne, A. G. & Smith, F. G. 1989 *Mon. Not. R. Astron. Soc.* **237**, 533.

Mestel, L. 1994 In *Cosmical magnetism* (ed. D. Lynden-Bell), p. 181. Dordrecht: Kluwer.

Moss, D. 1998 *Mon. Not. R. Astron. Soc.* **297**, 860.

Neininger, N. 1992 *Astron. Astrophys.* **263**, 30.

Neininger, N. & Horellou, C. 1996 In *Polarimetry of the interstellar medium* (ed. W. G. Roberge & D. C. B. Whittet), p. 592. Astronomical Society of the Pacific.

Neininger, N., Klein, U., Beck, R. & Wielebinski, R. 1991 *Nature* **352**, 781.

Neininger, N., Beck, R., Sukumar, S. & Allen, R. J. 1993 *Astron. Astrophys.* **274**, 687.

Niklas, S. 1995 PhD thesis, University of Bonn.

Niklas, S. & Beck, R. 1997 *Astron. Astrophys.* **320**, 54.

Patsis, P. A., Grosbol, P. & Hiotelis, N. 1997 *Astron. Astrophys.* **323**, 762.

Reuter, H.-P., Krause, M., Wielebinski, R. & Lesch, H. 1991 *Astron. Astrophys.* **248**, 12.

Reuter, H.-P., Klein, U., Lesch, H., Wielebinski, R. & Kronberg, P. P. 1994 *Astron. Astrophys.* **282**, 724.

Rohde, R. & Elstner, D. 1998 *Astron. Astrophys.* **333**, 27.

Rohde, R., Beck, R. & Elstner, D. 1999 *Astron. Astrophys.* **350**, 423.

Ruzmaikin, A., Sokoloff, D., Shukurov, A. & Beck, R. 1990 *Astron. Astrophys.* **230**, 284.

Schoofs, S. 1992 Diploma thesis, University of Bonn.

Segalovitz, A., Shane, W. W. & de Bruyn, A. G. 1976 *Nature* **264**, 222.

Shukurov, A. 1998 *Mon. Not. R. Astron. Soc.* **299**, L21.

Soida, M., Urbanik, M. & Beck, R. 1996 *Astron. Astrophys.* **312**, 409.

Soida, M., Urbanik, M., Beck, R. & Wielebinski, R. 1999 *Astron. Astrophys.* **345**, 461.

Sokoloff, D. D., Shukurov, A. & Krause, M. 1992 *Astron. Astrophys.* **264**, 396.

Sokoloff, D. D., Bykov, A. A., Shukurov, A., Berkhuijsen, E. M., Beck, R. & Poezd, A. D. 1998 *Mon. Not. R. Astron. Soc.* **299**, 189 (Erratum **303**, 207).

Sukumar, S. & Allen, R. J. 1989 *Nature* **340**, 537.

Sukumar, S. & Allen, R. J. 1991 *Astrophys. J.* **382**, 100.

Urbanik, M., Elstner, D. & Beck, R. 1997 *Astron. Astrophys.* **326**, 465.

van Albada, G. D. & van der Hulst, J. M. 1982 *Astron. Astrophys.* **115**, 263.

von Linden, S., Otmianowska-Mazur, K., Lesch, H. & Skupniewicz, G. 1998 *Astron. Astrophys.* **333**, 79.

Wielebinski, R. & Krause, F. 1993 *Astron. Astrophys. Rev.* **4**, 449.

Discussion

T. G. Forbes (*EOS Institute, The University of New Hampshire, USA*). In your 6 cm image of M31 there is a field signature in the nucleus which you didn't discuss. Is this evidence for a unipolar field? If not, what is the structure of the field in the nucleus?

R. Beck. The central region of M31 hosts a mini-spiral, visible in optical line emission, driven by star formation activity. The magnetic field follows this structure, but we don't have Faraday rotation data yet to determine the polarity. This central field shows no connection to the outer 'ring'.

D. Moss (*University of Manchester, UK*). In the dynamo model with $m = 0$ and $m = 2$ fields presented, was this the superposition of two linear modes, or the result of a general nonlinear calculation, i.e. do the $m = 0$ and $m = 2$ fields exist stably in a nonlinear model?

R. Beck. Yes, in the nonlinear dynamo model for NGC 6946 by Rohde, Elstner and myself the $m = 0$ and $m = 2$ modes coexist so that 'magnetic arms' emerge. The $m = 1$ mode is suppressed due to the assumption of a two-armed spiral and the small correlation time in our model.

R. D. Davies (*Nuffield Radio Astronomy Laboratories, Macclesfield, UK*). Could you say something about the fractional polarization you have observed; clearly less in the arms and greater in the interarm regions? What are typical quantitative values?

R. Beck. The fractional polarization is up to 50% in interarm regions of many galaxies. Spiral arms with strong star formation regions have a few per cent between dense complexes (observed with 200–500 pc spatial resolution). Quiet spiral arms reveal moderate fractional polarizations (typically 5–20%).

G. Pooley (*University of Cambridge, UK*). You showed some examples where the polarized arms avoid the optical arms. Are you convinced that this is not just a Faraday depolarization effect? At 20 cm, depolarization is dominant; at 6 cm the Faraday depths are only about 10 times smaller.

R. Beck. We see the 'magnetic arms' in NGC 6946 at 3 cm and 6 cm wavelengths with similar structure and thus can exclude strong Faraday depolarization. We also can exclude the magnetic arms being a pure effect of varying field tangling (beam depolarization) because the magnetic arms are also visible in our maps of the total intensity.

D. W. Hughes (*University of Leeds, UK*). You associate the presence of a coherent magnetic field in galaxies with a dynamo-generated field. Is it obvious that galactic fields have to be dynamo generated? Bearing in mind the results of Vainshtein and collaborators that turbulent diffusion of magnetic fields in a highly conducting gas can be dramatically suppressed by the dynamical effects of the field, is it not conceivable that the fields observed are due to the motions of the gas in some initial field but may not need to be generated by a dynamo?

R. Beck. Sheared primordial fields cannot generate quadrupole (SO) fields as observed, e.g. in M31. As far as we know today, only the dynamo is able to do this.

F. Graham-Smith (*Jodrell Bank, University of Manchester, UK*). What evidence is there for your statement that there are no field reversals on a kpc scale other than in our galaxy?

R. Beck. The resolution and sensitivity of our observations are sufficient to detect such reversals but we didn't detect any. Using Faraday rotation measures between 3 and 6 cm, we are not affected by angle ambiguities. I believe that with more pulsar RM data in our galaxy more reversals will appear, which may be the signatures of a tangled field, not resolvable in external galaxies.

L. Mestel (*The University of New Hampshire, USA*). Subramanian and I studied the effect of an azimuth-dependent alpha effect, due to, for instance, a spiral density wave. We found that an α–Ω dynamo yields a spiral magnetic field with maxima systematically displaced from the density wave. The density wave is often supposed to trigger formation of stars, including the more massive stars that could lead to amplified turbulence. Can you comment on this picture?

R. Beck. Indeed, in your papers (Mestel & Subramanian 1991; Subramanian & Mestel 1993) you found, in the case of a non-axisymmetric alpha effect, that the magnetic spiral of the bisymmetric dynamo mode ($m = 1$) leads with respect to the density wave within the corotation radius and TRAILS outside, i.e. no displacement near corotation. As we didn't find any signature for a bisymmetric mode in NGC 6946, I would like to propose to study the evolution of the $m = 2$ dynamo mode in your model. In the recent model by Rohde *et al*. (2000), the alpha effect is also larger in the arms (due to a longer correlation time there), but the maximum displacement between magnetic field and gas occurs around the corotation radius. The magnetic field is more turbulent in the arms than in the interarm regions because the observed degree of polarization is low in the arms even at short observation wavelengths.

Additional references

Mestel, L. & Subramanian, K. 1991 *Mon. Not. R. Astron. Soc.* **248**, 677.
Subramanian, K. & Mestel, L. 1993 *Mon. Not. R. Astron. Soc.* **265**, 649.